Behavioral/Cognitive

REM Sleep Microstates in the Human Anterior Thalamus

Péter Simor,[1,2,3] Orsolya Szalárdy,[2,4] Ferenc Gombos,[5] Péter Przemyslaw Ujma,[2,6] Zsófia Jordán,[6] László Halász,[6] Loránd Erőss,[6] Dániel Fabó,[6] and Róbert Bódizs[2,4]

[1]Institute of Psychology, ELTE, Eötvös Loránd University, Budapest 1064, Hungary, [2]Institute of Behavioural Sciences, Semmelweis University, Budapest 1089, Hungary, [3]UR2NF, Neuropsychology and Functional Neuroimaging Research Unit at CRCN, Center for Research in Cognition and Neurosciences and UNI-ULB Neurosciences Institute, Université Libre de Bruxelles, Brussels 1050, Belgium, [4]Institute of Cognitive Neuroscience and Psychology, Research Centre for Natural Sciences, Budapest 1117, Hungary, [5]MTA-PPKE, Hungarian Academy of Sciences, Pázmány Péter Catholic University, Adolescent Development Research Group, Budapest 1088, Hungary, and [6]National Institute of Clinical Neurosciences, Budapest 1145, Hungary

Rapid eye movement (REM) sleep is an elusive neural state that is associated with a variety of functions from physiological regulatory mechanisms to complex cognitive processing. REM periods consist of the alternation of phasic and tonic REM microstates that differ in spontaneous and evoked neural activity. Although previous studies indicate, that cortical and thalamocortical activity differs across phasic and tonic microstates, the characterization of neural activity, particularly in subcortical structures that are critical in the initiation and maintenance of REM sleep is still limited in humans. Here, we examined electric activity patterns of the anterior nuclei of the thalamus as well as their functional connectivity with scalp EEG recordings during REM microstates and wakefulness in a group of epilepsy patients ($N = 12$, 7 females). Anterothalamic local field potentials (LFPs) showed increased high-α and β frequency power in tonic compared with phasic REM, emerging as an intermediate state between phasic REM and wakefulness. Moreover, we observed increased thalamocortical synchronization in phasic compared with tonic REM sleep, especially in the slow and fast frequency ranges. Wake-like activity in tonic REM sleep may index the regulation of arousal and vigilance facilitating environmental alertness. On the other hand, increased thalamocortical synchronization may reflect the intrinsic activity of frontolimbic networks supporting emotional and memory processes during phasic REM sleep. In sum, our findings highlight that the heterogeneity of phasic and tonic REM sleep is not limited to cortical activity, but is also manifested by anterothalamic LFPs and thalamocortical synchronization.

Key words: **connectivity; REM; sleep; synchronization; thalamus**

Significance Statement

REM sleep is a heterogeneous sleep state that features the alternation of two microstates, phasic and tonic rapid eye movement (REM). These states differ in sensory processing, awakening thresholds, and cortical activity. Nevertheless, the characterization of these microstates, particularly in subcortical structures is still limited in humans. We had the unique opportunity to examine electric activity patterns of the anterior nuclei of the thalamus (ANTs) as well as their functional connectivity with scalp EEG recordings during REM microstates and wakefulness. Our findings show that the heterogeneity of phasic and tonic REM sleep is not limited to cortical activity, but is also manifested in the level of the thalamus and thalamocortical networks.

Introduction

Rapid eye movement (REM) sleep is a fundamental neural state that seems to facilitate a variety of functions from basic physiological mechanisms (Lyamin et al., 2018) to complex cognitive processes (Boyce et al., 2016). REM sleep features the alternation of two distinct microstates: phasic and tonic REM. These substates differ with respect to spontaneous (Simor et al., 2019) and evoked cortical activity (Takahara et al., 2006), neuronal synchronization (Simor et al., 2018), and arousal thresholds (Ermis et al., 2010), suggesting that REM microstates might cover diverse neurophysiological mechanisms and functions within REM periods (Simor et al., 2020).

Previous studies focusing on REM microstates applied fMRI (Wehrle et al., 2007; Miyauchi et al., 2009), EEG (Jouny et al., 2000; Simor et al., 2019), in addition to a limited number of electrocorticographic (ECoG) analyses (e.g., De Carli et al., 2016). Despite the advantages of such techniques, the analyses of REM microstates and the interpretation of research findings raises

Received July 20, 2020; revised Dec. 24, 2020; accepted Feb. 10, 2021.

Author contributions: P.S. and R.B. designed research; P.S., O.S., Z.J., L.H., L.E., D.F., and R.B. performed research; P.S., O.S., F.G., P.P.U., Z.J., L.H., L.E., and D.F. analyzed data; P.S., O.S., F.G., and P.P.U. wrote the paper.

The work was supported by the National Research, Development and Innovation Office of Hungary Grant NKFI_FK_128100, K_128117, the ELTE Thematic Excellence Program 2020 TKP2020-IKA-05, and the Higher Education Institutional Excellence Program of the Ministry of Human Capacities in Hungary, within the framework of the Neurology thematic program of the Semmelweis University.

The authors declare no competing financial interests.

Correspondence should be addressed to Péter Simor at simor.peter@ppk.elte.hu.

https://doi.org/10.1523/JNEUROSCI.1899-20.2021

Copyright © 2021 the authors

many difficulties. External stimulation seems to suppress phasic REM (Wehrle et al., 2007); therefore, the study of phasic microstates is very challenging in the noisy MR environment. Scalp EEG and ECoG are powerful tools to record and analyze REM sleep, but are not able to uncover the electric activity of subcortical structures that are critical in the initiation and maintenance of REM sleep (Luppi et al., 2011).

We aimed to overcome these methodological difficulties by analyzing electric activity patterns of phasic and tonic REM in a group of epilepsy patients that were implanted with electrodes in the anterior nuclei of the thalamus (ANTs). The ANT, because of its relationship with the subiculum, and the mammillary bodies, and its reciprocal connections with the anterior cingulate and medial frontal cortex (Child and Benarroch, 2013; Ketz et al., 2015), is an important structure among the frontolimbic neural pathways that orchestrate REM sleep (Muzur et al., 2002; Miyauchi et al., 2009; Luppi et al., 2011). Accordingly, the ANT appears to be a critical node that transmits subcortical activation patterns to cortical regions (Gonzalo-Ruiz et al., 1995; Vertes et al., 2001; Child and Benarroch, 2013; Ketz et al., 2015; Renouard et al., 2015), and may contribute to the emotional and mnemonic functions of REM sleep (Walker, 2009).

The activity of the ANT is particularly relevant with respect to REM microstates. Tonic REM is clearly distinguishable from phasic REM by increased cortical high-α and β frequency power (De Carli et al., 2016; Simor et al., 2019) that seems to reflect enhanced arousal and environmental alertness compared with phasic REM periods when the brains appears to be disconnected from the surrounding environment (Simor et al., 2020). In resting wakefulness, the increase in α and β EEG power was associated with the activity of a cingulo-insular-thalamic network that maintains arousal and facilitates alertness (Sadaghiani et al., 2010). Since the ANT forms part of the cholinergic ascending reticular activating system modulating arousal in wakefulness (Liu et al., 2012), it potentially contributes to increased arousal-related activity in tonic REM sleep. Therefore, our first aim was to examine frequency-specific activity to examine whether α and β power was increased in tonic versus phasic REM in the level of the ANT.

Phasic REM periods are characterized by the activity of a thalamocortical network including limbic and paralimbic areas (Wehrle et al., 2007; Miyauchi et al., 2009), and increased cortical synchronization in the δ (~2 Hz) and γ (30–48 Hz) frequency ranges (Simor et al., 2019). Although the latter were measured on the level of the scalp, electric activity within the δ and γ range were both observed in limbic areas (amygdala and hippocampus) during REM sleep (Bódizs et al., 2001; Corsi-Cabrera et al., 2016). Since the ANT is part of the limbic system, our second aim was to corroborate the relative enhancement of thalamocortical activity in phasic REM sleep by measuring functional connectivity between the ANT and the cortex (i.e., scalp) in phasic versus tonic REM.

Materials and Methods

Participants

We analyzed the data of 12 epilepsy patients (M_{age} = 35.33, range: 17–64; 7 females) undergoing ANT deep brain stimulation (DBS) treatment protocol in the National Institute of Clinical Neurosciences, Budapest, Hungary. Patients were included in the study if they had at least one night of co-registered ANT local field potentials (LFPs) and scalp EEG/polygraphy, as well as a sufficient amount of phasic and tonic REM sleep segments within their nocturnal recordings. Of the available 15 co-registered ANT-EEG/polygraphy records, 12 contained at least 5 min of unequivocal segments of distinct phasic and tonic REM sleep. The local ethical committee of the National Institute of Clinical Neurosciences approved the research protocol. Participants signed informed consent for taking part in the study.

Procedures

Surgical procedures

Medtronic DBS electrodes were stereotaxically inserted bilaterally in the anterior part of the thalamus in a state of general anesthesia to reduce seizures in pharmacoresistant, surgically non-treatable epilepsy patients. Besides frontal transventricular (nine patients) and extraventricular trajectories (three patients: two patients having contacts in the left side, and one patient with a contact in the right side), the posterior parietal extraventricular approaches (two patients) were used in accordance with the decisions of the clinical-neurosurgical team.

Individual contact localization

Preoperative MRI and postoperative CT images were co-registered using tools available in the FMRIB Software Library (FSL, Oxford, FLIRT, linear registration, 6 df) to ensure the individualized localization of thalamic contacts. Threshold has been applied on the co-registered CT scans to achieve the desired level of density for proper identification of the lead, thus removing the surrounding brain tissue. Coordinates of the most distal point of the lead has been identified and a more proximal point has been selected along the line of the contacts to mathematically reconstruct the coordinates of the center point of each contact using Euclidean distance in three-dimensional space. These points superimposed over the T1 MRI image provided a guideline for contact localization by examining their location to the anatomic boundaries of the ANT (Fig. 1). Anatomical positions according to standard coordinates of the contacts were double-checked by using the mamillothalamic tract as an anatomic guide to localize the ANT. In case of convergent results of these two methods, the ANT contacts were considered as subjects for further digital signal processing in the present study (see below). Out of 12 patients, we identified six patients that had been successfully implanted with electrodes in one side of the ANT, and six patients that had electrodes in both sides of the ANT.

Recordings

DBS electrodes were externalized and connected to the EEG headbox/amplifier. Electrophysiological and video recordings were performed by using an SD-LTM 64 Express EEG/polygraphic recording system and the System Plus Evolution software (Micromed). Physiologic signals were recorded at 8192 Hz/channel effective sampling rate with 22-bit precision and hardware input filters set at 0.02 (high pass: 40 dB/decade) and 450 Hz (low pass: 40 dB/decade). Data were decimated by a factor of four by the firmware resulting in stored time series digitized at 2048 Hz/channel. LFPs of the ANT were assessed by bilateral (L, left; R, right) quadripolar electrodes (LTh0, LTh1, LTh2, LTh3, RTh8, RTh9, RTh10, RTh11) according to a bipolar reference scheme: LTh0-LTh1, LTh1-LTh2, LTh2-LTh3, LTh0-LTh3, RTh8-RTh9, RTh9-RTh10, RTh10-RTh11, RTh8-RTh11. LTh0-LTh3 and RTh8-RTh11 were the distant reference derivations on the left and the right side of the ANT, respectively. Scalp EEG was recorded at electrode placements according to the 10–20 system (Fp1, Fp2, Fpz, F3, F4, F7, F8, C3, C4, T3, T4, T5, T6, P3, P4, O1, O_2, Oz; Jasper, 1958) extended with the inferior temporal chain (F9, F10, T9, T10, P9, P10; Rosenzweig et al., 2014) and additional two anterior zygomatic electrodes (ZA1, ZA2; Manzano et al., 1986). EEG signals were re-referenced offline to the mathematically linked T9 and T10 points [(T9 + T10)/2]. Ocular movements were assessed by the ZA1-ZA2 bipolar record created by off-line re-referencing, and submental electromyograms (EMGs) were recorded by bipolarly referenced electrodes placed on the chin. Electrocardiographic activity was recorded by an electrode placed at the midclavicular line on the left and the fifth intercostal space referred to the CP1 location on the scalp. Two patients (#1, #2) were set up with atypical electrode montages, slightly differing from the ones described above. Record of Patient #3 contained no Fpz, P9, P10, and EMG time series, while in the case of patient #2 F3, F4, C3,

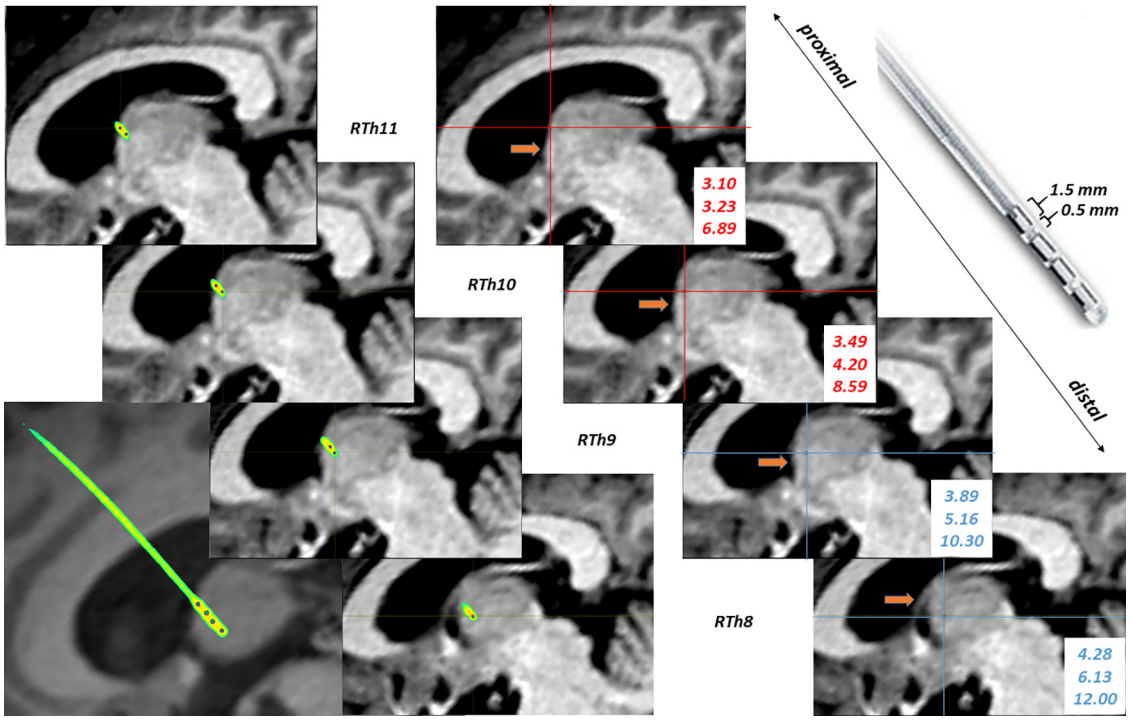

Figure 1. Saggital view of right-hemispheric thalamic contacts in patient #6. Parallel series of images are preoperative MRI-postoperative CT fusions showing the locations of the Medtronic electrode in the brain (left) and successive electrode contact locations based on standard coordinates (measured position of electrode contacts with respect to Mid Commissural Point in mm, left). Red cross-hairs indicate ANT-contacts, whereas blue ones are outside of the ANT (in the mediodorsal nucleus of the thalamus). Brown arrow: tractus mamillothalamicus. Left bottom image is a preoperative MRI-postoperative CT fusion in a skewed plane highlighting all right-side contacts in a single view. Right upper corner: enlarged image of the electrode with contact and intercontact lengths indicated in mm.

C4, P3, and P4 were missing, although Pz was present in this latter case. Missing contacts were treated as missing values in the statistical analyses.

Data preprocessing

Continuous video-EEG recordings were acquired after the operation and the nocturnal recordings we analyzed were initiated ~10 h after the implantation of ANT electrodes. The continuous recordings were automatically segmented into chunks of 90 min by the recording software. As there were no explicit lights off and lights on time during monitoring (patients were free to decide when they went to sleep), we marked the first and the last chunk of the nocturnal recordings (between 7 P.M. and 9 A.M.) for each subject. In order to assure that the first and the last chunks belonged to the period that patients were supposed to spend asleep, the first 90 min chunk was required to contain at least 10 min of continuous sleep in the second half of the recording (indicating sleep onset). Likewise, the last chunk was required to contain at least 10 min of continuous sleep in the first half (indicating sleep before awakening). If these criteria were fulfilled, the respective chunks were considered as the beginning and the final segments of the sleep session, and hence the first and the last chunks, as well as all the periods in between were considered as nocturnal sleep records, and were concatenated into a single file for further analyses. Sleep staging was performed manually with a custom-made software tool developed for all-night EEG data analysis (FercioEEGPlus, Ferenc Gombos, 2008–2020). Sleep sategs were scored according to standardized criteria of the American Academy of Sleep Medicine (AASM) by an expert trained in sleep research (Berry et al., 2012). All epochs scored as REM sleep were considered for further analyses. (The duration of periods scored as REM sleep is presented separately for each participant in Table 1.) Phasic and tonic segments from all epochs scored as REM sleep were categorized by visual inspection based on the presence or absence of a burst of eye movements. Four-second-long segments were coded as phasic REM when the EOG channel showed at least two consecutive eye movements that lasted <500 ms and exhibited 100 μV (or larger) amplitudes within the specific time window. Previous studies used less conservative amplitude criteria to identify EMs (Tan et al., 2001; Darchia et al., 2003); however, eye movements in bipolar EOG montages produce higher amplitudes; therefore, we restricted our analyses to relatively larger eye movements. The criterion for the duration of EMs was based on earlier studies indicating that EMs during REM do not exceed 2 Hz in terms of frequency (Tan et al., 2001; Darchia et al., 2003). Four-second-long segments without significant bursts of eye movements (EOG deflection of <25 μV) were categorized as tonic REM. The selection of segments were conducted by research assistants trained in sleep scoring, and the selected 4-s-long periods were visually inspected by a trained sleep researcher to exclude segments with inaccurate categorizations. In order to increase the stationarity of the data, we further segmented the 4-s phasic and tonic epochs into 2-s-long trials with 50% overlap. Finally, the new segments were visually inspected to discard trials showing movement-related and technical artifacts or periods with inter-ictal spikes or signs of pathologic activity, yielding 376.8 ± 302.21 (range: 69–1154) phasic REM, and 624.83 ± 326.06 (range: 102–1106) tonic REM trials.

To compare REM microstates with resting wakefulness, 10 min of eyes-closed wakefulness were selected from a subset of participants (N = 9) in which artifact-free awake periods were available. (Awake periods included a large number of movement-related artifacts in our sample). We selected awake segments from presleep wakefulness and from periods of wake after sleep onset throughout the night. Preprocessing steps of awake trials were identical to those performed on REM trials, yielding to an average number of 273.33 ± 61.95 (range: 181–390) awake trials.

Data and statistical analyses

Data analyses were performed in MATLAB (version 9.3.0.713579, R2017b, The MathWorks) using the Fieldtrip open source toolbox (Oostenveld et al., 2011). We computed the power spectral densities of Hanning-tapered 2-s-long trials by applying the Fast Fourier Transform routine on the signals extracted from the available ANT records. Bin-wise spectral power between 1.5 and 48 Hz was obtained with 0.5-Hz resolution and averaged across trials for phasic and tonic REM sleep. If the

Table 1. Sleep architecture of the night records of the subjects involved in the study (all measures are expressed in minutes)

Patient	Total recording time	Sleep duration	WASO	Wake	S1	S2	S3	REM
#1	690.3	416	187	274.6	59.3	226.7	38.7	91.3
#2	596	542.3	29.6	53.7	45.3	312	66.7	118.3
#3	662.6	247.7	92.3	415	62	146.3	0	39.3
#4	503	461.3	38.7	41.7	10	296.7	86	68.7
#5	450	397	29.3	53	24	168	82.7	122.3
#6	450	347.3	76.3	102.7	26.3	274.3	14.3	32.3
#7	450	294.3	155.6	155.7	34	174.3	20	66
#8	630	522	88.7	108	19	420.7	16.7	65.7
#9	720	574.3	56.7	145.7	15.7	433.3	53.3	72
#10	630	493.3	119.3	136.7	25.7	386.3	36.3	45
#11	576.6	425.3	132.3	151.3	158.7	234.3	0	32.3
#12	600	560	30	40	47	295.7	98	119.3
Mean (SD)	579,9 (95,81)	440.1 (105.5)	86.17 (53.34)	139.8 (109.2)	43.92 (39.83)	280.7 (96.2)	42.72 (34.27)	72.72 (33.46)

As there were no explicit schedules of lights off, we did not analyze sleep latency and sleep efficiency.
WASO, wake after sleep onset refers to wake time after the first epoch of not S1 sleep.

patient had two available records within the ANT (bilaterally), we used the average of the spectral power densities of the two signals. For those who had only one available channel, the average spectral power density of that single channel was considered. This way, for each patient we extracted the average spectrogram for phasic and tonic REM sleep. Bin-wise spectrograms of phasic and tonic REM sleep were contrasted by permutation tests suitable to analyze EEG time series (De Gennaro et al., 2000; Maris and Oostenveld, 2007; Tarokh et al., 2010). In brief, we used two-sided paired t tests to examine the differences between phasic and tonic REM spectral power values in each frequency bin. In order to evaluate statistical significance, the observed t values were compared against the distribution of t values obtained from 5000 samples where phasic and tonic states were randomly shuffled. Statistical significance was set to $p < 0.05$. Non-parametric permutation statistics is an efficient way to analyze spectral power without making prior assumptions regarding the distribution of the data. Nevertheless, since we contrasted phasic and tonic REM states in each frequency bin, we had to consider the issue of multiple comparisons. In order to attenuate type-1 error because of multiple comparisons, we followed the criteria introduced by Tarokh and colleagues (Tarokh et al., 2010) considering specific frequency bins significant if at least three adjacent bins reached the statistical threshold. Since we used a frequency resolution of 0.5 Hz, the probability to obtain three adjacent frequency bins reaching statistical significance by chance is low (Tarokh et al., 2010). Single bins showing ps < 0.05 were visualized but were not considered as statistically significant. We applied the same procedure for analyzing spectral power in resting wakefulness.

Thalamocortical synchronization was assessed by the phase locking value (PLV; Lachaux et al., 1999) and the weighted phase lag index (WPLI; Vinck et al., 2011) scores as implemented in the MATLAB Fieldtrip toolbox (Oostenveld et al., 2011). We focused on these measures as both quantify the consistency of frequency-specific phase differences between two signals regardless of changes in amplitude. Whereas the WPLI disregards random and zero (or π) phase-angle differences, and hence it is immune to the influence of volume conduction and common sources, the PLV is not absolutely devoid of such effects. (WPLI attenuates the effect of phase differences that fluctuate around zero or π, whereas PLV is only immune phase differences at zero or π.) On the other hand, although the usage of the WPLI largely reduces false positives, real coupling between signals might be overlooked by the WPLI when phase differences are consistently small (Cohen, 2015). Therefore, the two measures can be considered as complementary to each other.

The complex cross-spectral densities of the ANT and scalp channel pairs were obtained by Fourier Transformation for each frequency bin (1.5–48 Hz, 0.5-Hz resolution) in each Hanning-tapered 2-s-long trial. PLV and WPLI between the ANT signal and all the available scalp electrodes were averaged in each participant for phasic REM, tonic REM and wakefulness. That is, PLV and WPLI scores of all channel pairs (ANT–Fp1, ANT-Fp2, ANT-F8, ANT-Fpz, ANT-Cz, ... ANT-O1, ANT-O2) available in the patients data were averaged. If the participant had two ANT recordings (six out of 12 patients had ANT electrodes in each side of the ANT, whereas in the other half of our sample, ANT recordings were only available in one side of the ANT), both sets of channel combinations (e.g., ANT1-Fp1, ANT2-FP1, ... ANT1-O_2, ANT2-O_2) were included in the averaged PLV and WPLI scores. Since we did not have a specific hypothesis regarding the frequency ranges of interest (like in case of high α-β spectral power), bin-wise averages of PLV and WPLI values were summed up to the consensual frequency bands of δ (1.5–4 Hz), θ (4.5–8 Hz), α (8.5–14 Hz), β (14.5–30 Hz), and γ (30.5–48 Hz) ranges, but bin-wise values were also retained for visualization purposes. Condition (phasic vs tonic) × band repeated measures ANOVA models (with Greenhouse–Geisser correction if the assumption of sphericity was violated), and *post hoc* comparisons (paired t tests or if normal distribution was not met Wilcoxon signed-rank tests) were evaluated for PLV and WPLI scores. Since *post hoc* tests were evaluated for each frequency band, p values were adjusted for multiple comparisons using a false discovery rate correction procedure described by Benjamini and Hochberg (Benjamini and Hochberg, 1995). The same analyses were performed to contrast PLV/WPLI in wakefulness and REM microstates in a subset of participants ($N = 9$).

Results

Sleep architecture

The distribution of sleep stages as well as conventional indices of sleep architecture are detailed in Table 1.

Increased high-α and β power in tonic versus phasic REM sleep in the ANT

As shown in Figure 2, tonic REM periods exhibited a relative increase in spectral power within the high-α and β frequency ranges compared with phasic REM periods: significant ($p <$ 0.05) frequency bins were observed between 9.5 and 18.5 Hz (Cohen's d values for significant bins ranged between 0.7 and 1.2). This finding indicates that the ANT exhibits increased activity in the high-α and β frequency ranges and may contribute to increased vigilance and arousal during tonic compared with phasic REM periods.

We compared spectral power in REM microstates with spectral in wakefulness in a subset of our participants ($n = 9$) in whom we could identify at least 10 min of clean (artifact-free) segments of eyes-closed, resting wakefulness. Tonic REM periods appeared as an intermediate state between phasic REM and wakefulness (Fig. 3). Spectral power in wakefulness was increased compared with phasic REM in frequency bins between 7–8.5 and 12.5–14.5 Hz (p values < 0.05, Cohen's d values: 0.7–1.26). None of the frequency bins were significantly different between tonic REM and wakefulness. (This subset of patients did

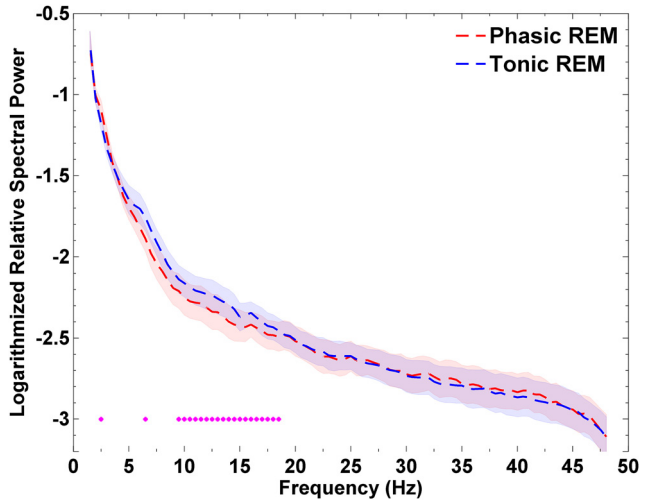

Figure 2. Spectral power of local field potentials (LFPs) recorded from the anterior nucleus of the thalamus (ANT) during phasic and tonic REM microstates in 12 epilepsy patients. Tonic REM periods showed relatively increased oscillatory activity in the high-alpha and beta frequency ranges between 9.5 and 18.5 Hz. Frequency bins below the statistical threshold ($p < 0.05$) are illustrated by magenta colored circles. Note that frequency bins were considered significant if at least three adjacent bins reached the threshold. Single bins below the threshold are also marked, but are not considered as significant. Shaded areas indicate standard errors. Permutation tests were carried out on non-normalized power spectra, but values are represented on a normalized (relative spectra) and logarithmic scale for visualization purposes.

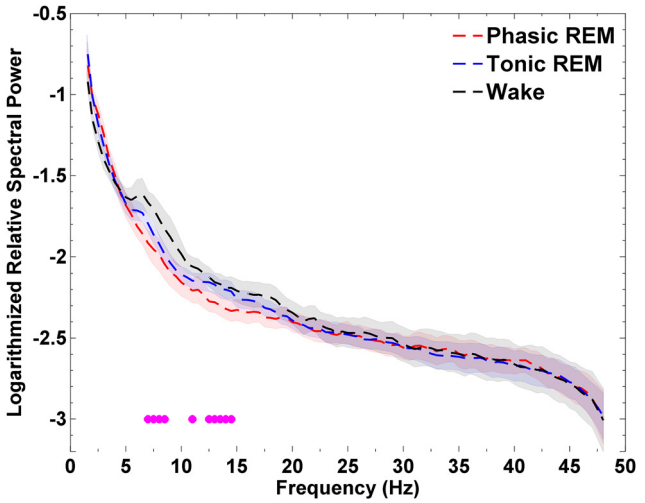

Figure 3. Spectral power of local field potentials (LFPs) recorded from the anterior nucleus of the thalamus (ANT) during phasic and tonic REM microstates and resting wakefulness in epilepsy patients ($n = 9$). Tonic REM sleep appeared as an intermediate state between phasic REM and wakefulness with respect to alpha and beta frequency power. Magenta colored circles mark significant ($p < 0.05$) differences between phasic REM and wakefulness. (No significant bins emerged between tonic REM and wakefulness.) Note that frequency bins were considered significant if at least three adjacent bins reached the threshold. Single bins below the threshold are also marked, but are not considered as significant. Shaded areas indicate standard errors. Permutation tests were carried out on non-normalized power spectra, but values are represented on a normalized (relative spectra) and logarithmic scale for visualization purposes.

not differ from the whole sample with respect to spectral power in phasic vs tonic REM, as tonic REM in this subsample also showed increased values between 12.5 and 18.5 Hz compared with phasic REM sleep.)

In order to examine whether the pattern of spectral power observed in the ANT in our group of patients is also apparent on the level of the scalp, the averaged power spectra of the parietal electrodes (because of the posterior peak of α activity) was juxtaposed to the power spectra of the ANT. Both values were normalized to visualize them on the same scale. The parietal EEG spectra of phasic and tonic REM sleep paralleled the pattern observed in the ANT LFPs, and was in line with previous findings on healthy participants (Jouny et al., 2000; Simor et al., 2016) with respect to increased tonic α and β power. The correspondence between the LFPs of the ANT and the scalp EEG measurements was also prominent in the state of resting wakefulness: the EEG α peak around 8 Hz was also visible (although to a much lesser extent) in the ANT (see Fig. 4).

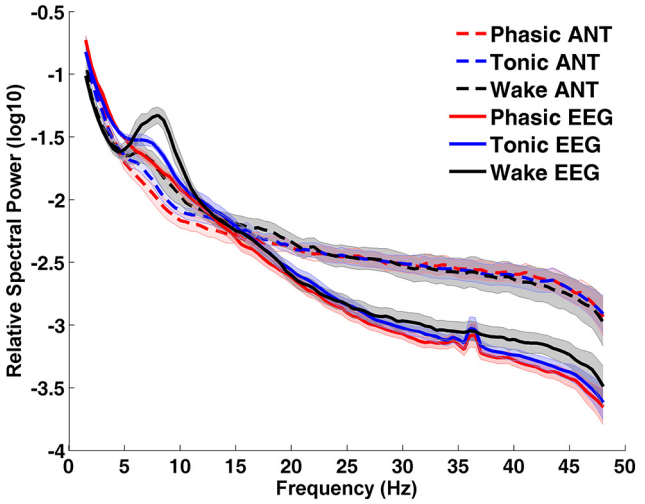

Figure 4. Spectral power in the ANT and the scalp during REM microstates and wakefulness ($N = 9$). Spectral power values are normalized by applying the relative spectra in order to represent spectral power densities of ANT and scalp recordings on the same scale. Logarithmic transformation was used to better visualize oscillatory activity in different frequencies. Scalp EEG power refers to the average of parietal electrodes. We selected parietal electrodes, since alpha activity is maximal on those sites.

Enhanced ANT-Scalp EEG synchronization in phasic compared with tonic REM

In order to examine thalamocortical network activity in REM microstates and to verify whether thalamocortical synchronization increases in phasic compared with tonic REM, we analyzed phase synchronization between the ANT and the scalp EEG recordings (averaged across all available electrodes; see Materials and Methods). Repeated measures ANOVAs models were used to contrast phase synchronization across the two conditions (phasic vs tonic) in five frequency bands (δ, θ, α, β, and γ). The ANOVA model revealed a main effect for Band in both synchronization indices (PLV: $F_{(44,4)} = 12.98$, $p < 0.001$, partial $\eta^2 = 0.54$; WPLI: $F_{(44,4)} = 14.82$, $p < 0.001$, partial $\eta^2 = 0.57$). More importantly, we observed a main effect of condition in case of the PLV ($F_{(11,1)} = 11.53$, $p = 0.006$, partial $\eta^2 = 0.51$), and the WPLI ($F_{(11,1)} = 11.99$, $p = 0.005$, partial $\eta^2 = 0.52$). *Post hoc* tests indicated this effect to be driven by increased PLV and WPLI in phasic compared with tonic REM, particularly in the slow and the fast frequency bands (Fig. 5). More specifically, δ, β, and γ bands showed significantly higher PLV and WPLI values in phasic compared with tonic REM sleep (Table 2). In addition, the interaction between condition and band was not significant in case of the PLV ($F_{(1.9,21)} = 1.43$, $p = 0.26$, partial $\eta^2 = 0.11$), and the WPLI ($F_{(15.47,1.4)} = 2.65$, $p = 0.11$, partial $\eta^2 = 0.19$) either. In sum, we observed increased functional synchronization between

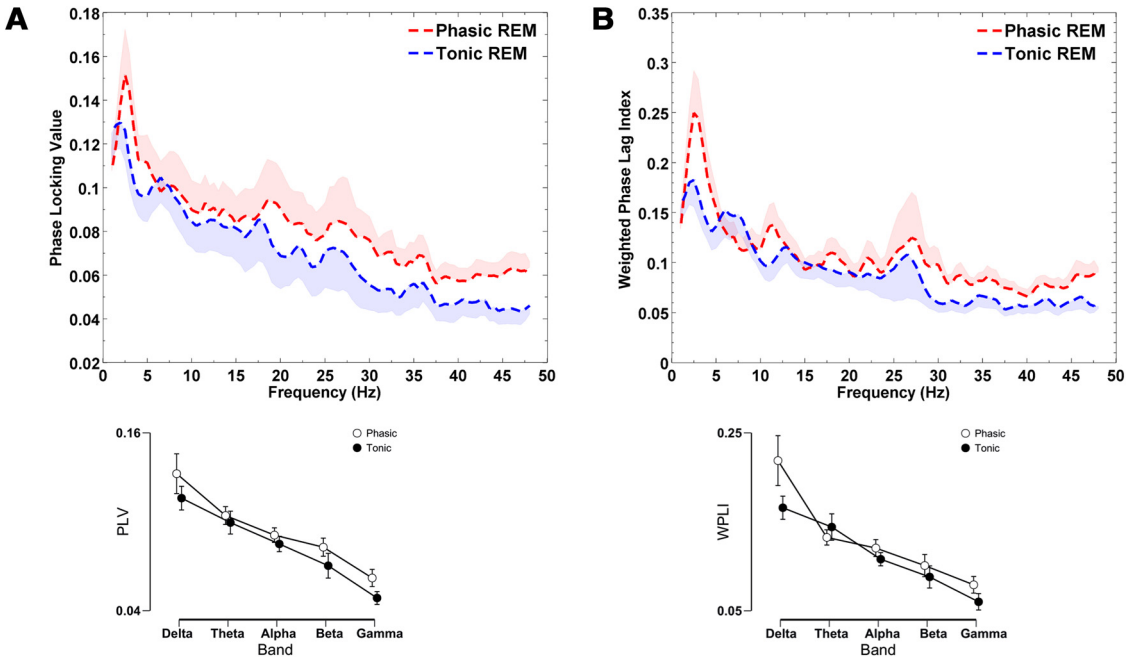

Figure 5. Thalamocortical connectivity as assessed by the (***A***) PLV and (***B***) WPLI between the ANT LFPs and scalp EEG signals in epilepsy patients ($n = 12$). Phasic compared with tonic REM sleep was characterized by increased PLV and WPLI scores as revealed by a main effect of condition in the condition × frequency band repeated measures ANOVA model (PLV: $F_{(11,1)} = 11.53$, $p = 0.006$, partial $\eta^2 = 0.51$; WPLI: $F_{(11,1)} = 11.99$, $p = 0.005$, partial $\eta^2 = 0.52$). Increased functional connectivity in the phasic REM period was observed in the δ, β, and γ bands in case of the PLV and WPLI. PLV and WPLI scores were obtained by averaging all combinations of ANT and Scalp EEG channel pairs. The upper figures illustrate bin-wise indices of functional connectivity in REM microstates, and the lower graphs show functional connectivity scores averaged across frequency bands. Shaded regions (in the bin-wise illustration, upper part) and vertical bars (in the band-wise illustration, lower part) represent SEs. In case of the bin-wise illustration, only the upper half of the SEs in phasic, and the lower half of the SEs in tonic REM were visualized. A smoothing moving average filter (spanning four data points) was applied to aid visualization.

the LFPs of the ANT and the scalp EEG signals during phasic in comparison with tonic REM periods.

Region-specific aspects of increased thalamocortical synchronization in phasic REM

In order to explore the region-specific patterns of synchronization between the ANT and scalp EEG channels, we performed *post hoc* analyses, focusing on the three frequency bands (δ, β, and γ) that showed significant differences across phasic and tonic REM states. Therefore, we contrasted functional synchronization between the ANT and frontal (averaging ANT-Fp1, ANT-Fp2, ANT-F3, ANT-F4, ANT-F7, ANT-F8), centrotemporal (averaging ANT-C3, ANT-C4, ANT-T3, ANT-T4), and parietooccipital (averaging ANT-P3, ANT-P4, ANT-T5, ANT-T6, ANT-O1, ANT-O2) EEG channels. The two-way interaction of condition × region and the three-way interaction of condition × region × band were evaluated by repeated measures ANOVA models that were performed separately for PLV and WPLI scores. In case of the PLV, the interaction between condition and region was not ($F_{(2,22)} = 0.7$, $p = 0.51$, partial $\eta^2 = 0.06$), but the interaction term between condition × region × band was significant ($F_{(1.9,21)} = 8.96$, $p < 0.0001$, partial $\eta^2 = 0.45$). A similar, although less robust pattern emerged in case of the WPLI (condition × region: $F_{(2,22)} = 0.8$, $p = 0.46$, partial $\eta^2 = 0.06$; condition × region × band: $F_{(2,22)} = 3.14$, $p = 0.02$, partial $\eta^2 = 0.22$). In case of the PLV, the interaction was mainly because of a relatively lower difference between phasic and tonic REM in anterior compared with posterior δ synchrony, whereas γ synchrony showed an opposite pattern: increased synchronization in phasic REM was more prominent between ANT and frontal EEG channels. In sum, the relative increase in phasic PLV within the δ range showed a posteroanterior gradient, and the relative increase in phasic PLV within the β and γ bands exhibited an anteroposterior gradient. *Post hoc* comparisons and effect sizes are detailed in Table 3. In case of the WPLI, the posteroanterior gradient of relatively increased synchrony within the δ range in phasic REM was less evident, but the anteroposterior gradient of increased β and γ synchrony emerged in phasic versus tonic REM (see *post hoc* comparisons and effect sizes in Table 3 and region-specific differences in synchronization in Fig. 6).

Thalamocortical synchronization in REM microstates and wakefulness

PLV and WPLI was examined also in resting wakefulness ($n = 9$) to juxtapose functional connectivity during wake with the patterns observed in REM microstates. A relative increase in the α range differentiated wakefulness from phasic and tonic REM in case of the PLV (phasic vs wakefulness: $t_{(8)} = -3.39$, FDR-corrected $p = 0.03$, Cohen's $d = -1.13$; tonic vs wakefulness: $t_{(8)} = -4.11$, FDR-corrected $p = 0.01$, Cohen's $d = -1.37$). Regarding the WPLI, *post hoc* comparisons revealed no significantly different frequency bands across wakefulness and phasic REM (all FDR-corrected $p > 0.1$), whereas WPLI in the β and γ range was nominally reduced in tonic REM compared with wakefulness ($t_{(8)} = -2.56$ and -2.51, FDR-corrected $p = 0.075$ and $p = 0.075$, Cohen's $d = -0.85$ and -0.84 for the β and γ bands, respectively). No other frequency bands showed significant differences across the three vigilance states after the correction for multiple comparisons. Figure 7 illustrates frequency-specific synchronization on a bin-wise level across wakefulness and REM microstates. A clear peak in the α range could be observed in wakefulness, compared with both REM microstates with respect to the PLV and WPLI. Moreover, thalamocortical synchronization at fast frequencies in wakefulness appeared to fall

Table 2. *Post hoc* comparisons of ANT-Scalp EEG functional synchronization scores during phasic and tonic REM sleep

	PLV				WPLI			
Frequency bands	Phasic vs tonic mean (SD)		Test statistic and FDR-corrected *p* value	Effect size	Phasic vs tonic mean (SD)		Test statistic and FDR-corrected *p* value	Effect size
δ	0.137 (0.05)	0.11 (0.02)	2.68 **0.03**	0.43	0.224 (0.11)	0.166 (0.06)	2.48 **0.03**	0.71
θ	0.112 (0.05)	0.099 (0.04)	1.35 0.20	-0.077^{+}	0.159 (0.09)	0.161 (0.08)	−0.13 0.9	−0.04
α	0.091 (0.04)	0.086 (0.04)	0.98 0.34	0.45	0.118 (0.04)	0.109 (0.04)	0.33 0.46	0.3
β	0.085 (0.04)	0.072 (0.05)	2.81 **0.025**	0.82	0.101 (0.05)	0.086 (0.04)	3.16 **0.01**	0.91
γ	0.06 (0.03)	0.05 (0.03)	2.87 **0.025**	0.82	0.084 (0.03)	0.063 (0.03)	3.6 **0.01**	1.03

PLV, phase locking value; WPLI, weighted phase lag index; FDR, false discovery rate. Test statistic refers to paired *t* test, unless marked with asterisk that refers to Wilcoxon signed-rank test. Effect Size refers to Cohen's *d* values. Significant *post hoc* tests are highlighted in bold.

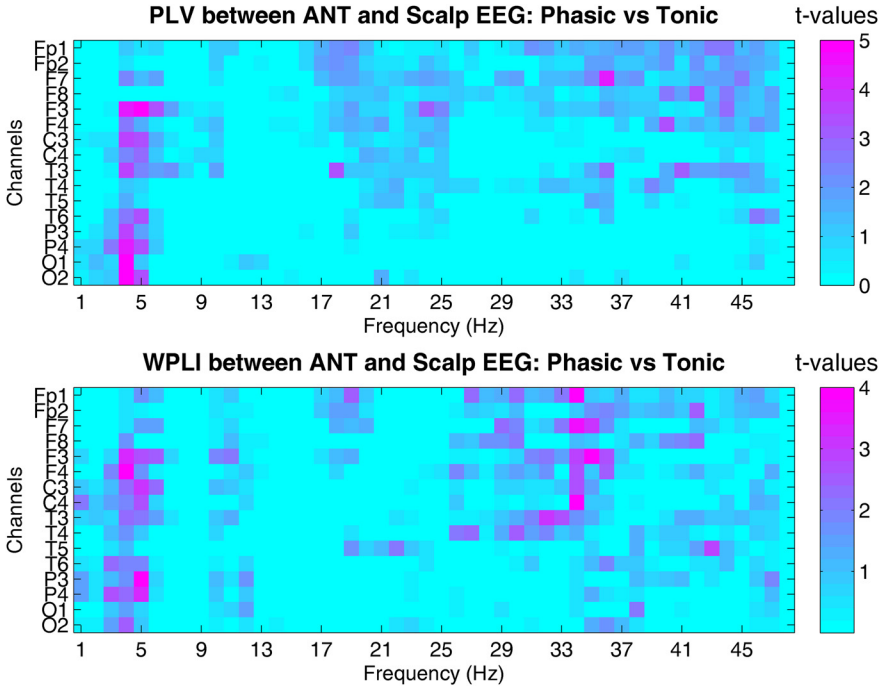

Figure 6. Region-specific aspects of thalamocortical synchronization across phasic and tonic REM microstates. The upper graph indicates bin-wise (1-48 Hz) statistical comparisons of Phase Locking Values (PLV) between phasic and tonic REM conditions in each frequency and thalamocortical (ANT and scalp EEG) channel pair. Color codes indicate paired samples t-tests across phasic and tonic conditions at each frequency and channel pair. The lower image shows the same analyses as above, but on the Weighted Phase Lag Index scores (WPLI). Thalamocortical synchronization shows increased values in phasic vs tonic REM within the delta, beta, and gamma frequency ranges by both metrics. The phasic increase in the delta band is more pronounced between the ANT and centro-parietal EEG channels, whereas the increase in beta and gamma synchrony shows an opposite pattern, that is, an antero-posterior gradient, peaking between ANT and frontopolar channel pairs.

in between the corresponding phasic and tonic values. In sum, thalamocortical synchronization appeared to be specifically increased in the α range during resting wakefulness in comparison with phasic and tonic REM microstates.

Discussion

We examined LFPs in the human ANT, as well as thalamocortical synchronization between the ANT and the cortex during the phasic and tonic microstates of REM sleep. REM microstates showed remarkable differences with respect to anterothalamic and thalamocortical activity based on the data of twelve epilepsy patients who were implanted with electrodes in the ANT. Enhanced high-α and β frequency power emerged in the ANT during tonic compared with phasic REM periods. On the other hand, we observed increased synchronization between the ANT LFPs and scalp EEG in phasic versus tonic REM, particularly in the slow (δ) and fast (β and γ) frequency ranges. Thalamocortical synchronization in resting wakefulness featured a prominent peak in the α range (~8 Hz), that was not apparent in REM microstates. To the best of our knowledge, our study is the first to examine the electrical activity of the human ANT in REM sleep, and to provide evidence on the heterogeneity of REM microstates in the level of the ANT and thalamocortical synchronization.

LFPs in the ANT across phasic and tonic REM microstates resemble previous findings that reported relatively increased α and β power during tonic REM in scalp EEG (Waterman et al., 1993; Jouny et al., 2000; Simor et al., 2016, 2019), and intracranial recordings of the motor (De Carli et al., 2016) and orbitofrontal cortices (Nishida et al., 2005). During resting wakefulness, high-α and β power (although the latter was less thoroughly examined) are considered to reflect a state of sustained alertness facilitating the anticipation of and the appropriate responses to task goals (Makeig and Inlow, 1993; Dockree et al., 2007). Several studies indicate that environmental alertness is indeed relatively increased in tonic compared with phasic REM. For instance, awakening threshold (Ermis et al., 2010) is lower and behavioral responsiveness (as measured by a button press in reaction to acoustic stimulation; Price and Kremen, 1980) is higher in tonic versus phasic REM. Moreover, event-related potentials (ERPs) elicited by abrupt changes embedded in a stream of auditory stimuli (rare stimuli embedded in frequent ones) are preserved to some extent during tonic but largely attenuated in phasic REM sleep (Sallinen et al., 1996; Takahara et al., 2002). More importantly, an instruction to specifically attend to the infrequent tone further increased the ERP differences between tonic and phasic REM, suggesting that attentional resources are more available during the tonic state (Takahara et al., 2006).

With respect to the neural correlates of high-α and β EEG activity during wakefulness, Sadaghiani and colleagues identified a widespread network, involving the dorsal anterior cingulate cortex, the anterior insula, the anterior prefrontal cortex, the thalamus, and the basal ganglia (Sadaghiani et al., 2010). A further study pinpointed that the anterior and mediodorsal nuclei

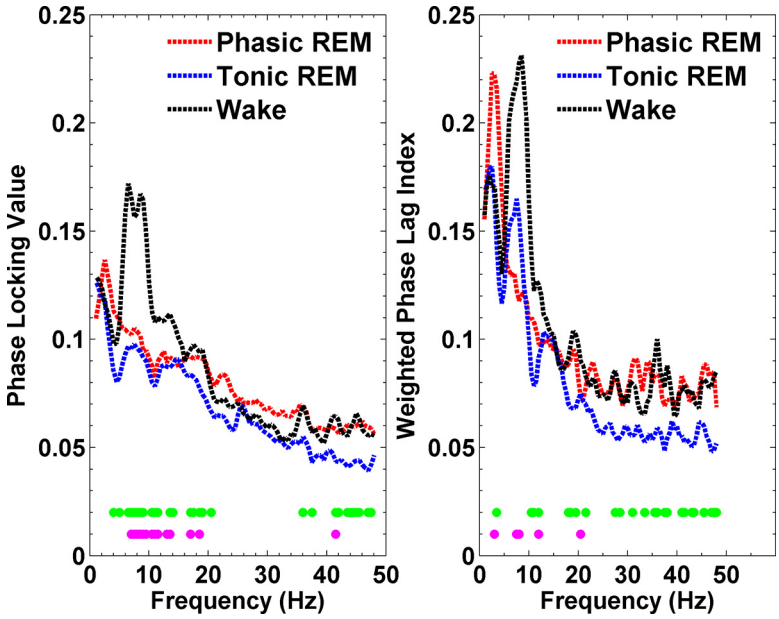

Figure 7. Thalamocortical connectivity quantified by the PLV and the WPLI between the ANT and scalp EEG signals in resting wakefulness and REM microstates. A large peak in the α range differentiates wakefulness from phasic and tonic REM microstates in case of both measures of neural coupling; $p < 0.05$ obtained by nonparametric permutation tests contrasting wakefulness versus phasic REM, and wakefulness versus tonic REM are marked by magenta and green circles, respectively. PLV and WPLI scores were obtained by averaging all combinations of ANT and Scalp EEG channel pairs.

Table 3. *Post hoc* comparisons of region-specific synchronization between phasic and tonic REM

	PLV		WPLI	
	t (FDR-*p*)	Cohen's *d*	*t* (FDR-*p*)	Cohen's *d*
δ Band				
ANT-frontal EEG	1.2 (0.13)	0.3452	2.2 (0.03)	0.6350
ANT-central EEG	2.6 (0.01)	0.7536	2.2(0.02)	0.6365
ANT-posterior EEG	4.1(0.0080)	1.1900	2.7(0.01)	0.7760
β Band				
ANT-frontal EEG	4.4 (0.0005)	1.2664	3.4 (0.003)	0.9751
ANT-central EEG	2.5(0.01)	0.7303	2.8 (0.008)	0.8223
ANT-posterior EEG	1.6 (0.07)	0.4705	1.8 (0.05)	0.5171
γ Band				
ANT-frontal EEG	4.5 (0.0004)	1.3020	4.12 (0.001)	1.1889
ANT-central EEG	2.1 (0.03)	0.6144	3.3 (0.004)	0.9449
ANT-posterior EEG	1.3 (0.1)	0.3853	2.7 (0.01)	0.7838

Statistical parameters and effects sizes indicate the phasic versus tonic contrasts in synchronization between the ANT and frontal, Central, and posterior scalp EEG channels, respectively.
t, paired samples *t* test; FDR-p, *p* values corrected by false discovery rate (Benjamini and Hochberg, 1995); PLV, phase locking value; WPLI, weighted phase lag index.

of the thalamus exhibited a positive blood oxygen level-dependent (BOLD) response linked to increased α EEG power (Liu et al., 2012). Interestingly, these nuclei were not functionally connected with the primary visual cortex (such as the posterior nuclei of the thalamus), but instead to the cingulate cortex, the cerebellum and the brainstem (Liu et al., 2012). Since these thalamic nuclei and the functionally connected areas overlap with the ascending arousal system, especially with its cholinergic projections (Saper et al., 2005), which are crucial in the generation of REM sleep (Datta and Siwek, 1997), it is plausible that this network modulates arousal and vigilance not exclusively during wakefulness (Liu et al., 2012), but presumably also during REM sleep. Accordingly, DBS of the ANT seems to increase arousals and sleep fragmentation probably because of the activation of the ascending arousal system (Voges et al., 2015). In line with the above, we suggest that relatively enhanced high-α and β power in the ANT reflects increased arousal facilitating environmental alertness during tonic REM periods. Accordingly, tonic REM spectral power in the ANT approached the levels observed in resting wakefulness, in accordance with previous findings that qualified tonic REM as an intermediate state in between phasic REM and wakefulness based on BOLD activity (Wehrle et al., 2007) and scalp EEG measurements (Sallinen et al., 1996; Takahara et al., 2002). Whether the ANT is part of the ascending arousal system, or has a causal effect on cortical neurons that support arousal and alertness is a question that should be addressed in future studies.

The other consistent finding in scalp EEG measurements, the increase in δ and γ power in phasic REM periods (Jouny et al., 2000; Simor et al., 2016, 2019; Bernardi et al., 2019) was not observed in the ANT. One possibility is that slow and fast frequency power in phasic REM originate from the synchronized activity of a large number of cortical ensembles, and therefore are not directly associated with LFPs of anterothalamic recordings.

On the other hand, the relative increase in slow and fast frequency activity during phasic (compared with tonic REM) was observed with respect to thalamocortical synchronization. Activity within the δ range and faster oscillatory activity within the β and γ frequency ranges exhibited increased phase synchronization between the ANT and the scalp in phasic versus tonic REM sleep. This finding in line with previous studies reporting the increased amount of slow and fast frequency cortical oscillations in relation to phasic REM activities (Frauscher et al., 2018; Bernardi et al., 2019; Simor et al., 2019), and indicate that neocortical interactions are key players in contributing to such activity. Although the network producing relatively increased synchronization in slow frequency activity during phasic REM remains elusive, Bernardi and colleagues (Bernardi et al., 2019) recently identified a cluster of 2.5- to 3-Hz frequency activity that was associated with eye movements (phasic REM) and exhibited neural sources in medial frontal regions. Based on the overlapping frequency range, on the link with eye movements, and on the identified neural sources (that are connected to the anterior thalamus), we may speculate that the cluster of δ activity identified by Bernardi et al. (2019) and our findings regarding increased thalamocortical synchrony in the δ range reflect the activity of overlapping neural networks.

The present findings also indicate that the increase in slow and fast frequency activity during phasic REM periods are not limited to corticocortical, but also involve thalamocortical interactions during phasic REM sleep. Since the ANT is part of the frontolimbic pathway, slow and fast frequency synchronization may reflect frontolimbic interactions. In animal studies, ($\sim$7 Hz) θ synchronization between limbic and cortical areas was specifically linked to the role of REM sleep in emotional memory processing (Hutchison and Rathore, 2015). The ANT has strong anatomic and functional connections with subcortical and frontolimbic structures (Child and Benarroch, 2013; Ketz et al., 2015), exhibits rhythmically

synchronous activity with limbic θ activity (Vertes et al., 2001), and appears to be strongly involved in mnemonic and emotional processes (Paré et al., 2002; Xiao and Barbas, 2002; Hartikainen et al., 2014; Sweeney-Reed et al., 2014; Ketz et al., 2015). Whereas limbic θ oscillations are predominant in the REM phase of rodents, studies suggest that the human analog of limbic θ power is an allometrically scaled, slower (1.5–3 Hz) rhythmic activity during REM sleep (Bódizs et al., 2001; Moroni et al., 2007, 2012). This frequency range overlaps with the slow δ peak (Fig. 6*A*,*B*) in thalamocortical synchronization we observed in phasic and to a lesser extent in tonic REM; therefore, we assume that slow frequency synchronization between the ANT and the scalp is related to the human limbic θ rhythm characteristic of REM sleep.

Thalamocortical synchronization in phasic REM also showed elevated values in fast frequency ranges. Increased γ activity in phasic REM was observed in scalp EEG (Abe et al., 2008), in intracerebral recordings, including the amygdala (Gross and Gotman, 1999; Corsi-Cabrera et al., 2016), and in high-density EEG originating partly from frontolimbic sources (Simor et al., 2019). In line with the assumption of a frontolimbic network involved in fast frequency activity, increased thalamocortical synchronization in phasic REM expressed an anteroposterior gradient showing relatively increased synchrony of the ANT with anterior EEG locations compared with synchrony of the ANT with posterior EEG channel pairs (Fig. 6).

Fast frequency activity was linked to emotional processing in wakefulness (Headley and Pare, 2013; Jabbi et al., 2015), and also in REM sleep (van der Helm et al., 2011). Since the ANT is part of the frontolimbic pathway, the synchronization of fast frequency bands between the ANT and scalp EEG signals might (partly) stem from the amygdala and related frontolimbic structures underlying emotional, perceptual processes that humans experience in the form of vivid dream images. Likewise, neuroimaging studies of REM sleep observed the enhanced activation of a thalamocortical network, involving the brainstem and frontolimbic areas on eye movements (phasic periods) during REM sleep (Wehrle et al., 2007; Miyauchi et al., 2009). Such network was assumed to provide the neural background of an emotional-perceptual-memory circuit producing intrinsic activity under attenuated external processing during phasic REM sleep (Wehrle et al., 2007).

It is important to note, that resting wakefulness featured a large α peak in thalamocortical synchronization that distinguished it from REM microstates. The same α peak (~8 Hz) emerged in the average power spectra of the scalp EEG and the ANT recordings during wakefulness. This pattern is in line with the findings indicating a temporal correlation between scalp (especially parietal) α power and BOLD positive responses in the anterior and mediodorsal thalamus during the awake state (Liu et al., 2012; Zotev et al., 2018). Although the peak in α power during tonic REM resembled the peak observed during wakefulness in both the ANT and the scalp (see S2), thalamocortical α synchronization apparent in wakefulness, but absent in REM indicates a larger involvement of cortical neurons in α oscillations during the awake state.

In sum, our findings put in evidence that the heterogeneity of phasic and tonic REM sleep is not limited to cortical activity, but is also manifested by anterothalamic LFPs and thalamocortical synchronization. The alternation of phasic and tonic periods might reflect the interplay between periods of intrinsically generated cognitive activity under sensory disconnection, and periods of partially reinstated attentional resources that facilitate environmental alertness.

References

Abe T, Matsuoka T, Ogawa K, Nittono H, Hori T (2008) Gamma band EEG activity is enhanced after the occurrence of rapid eye movement during human REM sleep. Sleep Biol Rhythms 6:26–33.

Benjamini Y, Hochberg Y (1995) Controlling the false discovery rate: a practical and powerful approach to multiple testing. J R Stat Soc Series B Stat Methodol 57:289–300.

Bernardi G, Betta M, Ricciardi E, Pietrini P, Tononi G, Siclari F (2019) Regional delta waves in human rapid eye movement sleep. J Neurosci 39:2686–2697.

Berry RB, Brooks R, Gamaldo CE, Harding SM, Marcus CL, Vaughn BV (2012) The AASM manual for the scoring of sleep and associated events. Rules, terminology and technical specifications. Darien: American Academy of Sleep Medicine. Available from http://www.aasmnet.org/resources/pdf/scoring-manual-preface.pdf.

Bódizs R, Kántor S, Szabó G, SzÃcs A, Erõss L, Halász P (2001) Rhythmic hippocampal slow oscillation characterizes REM sleep in humans. Hippocampus 11:747–753.

Boyce R, Glasgow SD, Williams S, Adamantidis A (2016) Causal evidence for the role of REM sleep theta rhythm in contextual memory consolidation. Science 352:812–816.

Child ND, Benarroch EE (2013) Anterior nucleus of the thalamus: functional organization and clinical implications. Neurology 81:1869–1876.

Cohen MX (2015) Effects of time lag and frequency matching on phase-based connectivity. J Neurosci Methods 250:137–146.

Corsi-Cabrera M, Velasco F, Del Río-Portilla Y, Armony JL, Trejo-Martínez D, Guevara MA, Velasco AL (2016) Human amygdala activation during rapid eye movements of rapid eye movement sleep: an intracranial study. J Sleep Res 25:576–582.

Darchia N, Campbell IG, Feinberg I (2003) Rapid eye movement density is reduced in the normal elderly. Sleep 26:973–977.

Datta S, Siwek DF (1997) Excitation of the brain stem pedunculopontine tegmentum cholinergic cells induces wakefulness and REM sleep. J Neurophysiol 77:2975–2988.

De Carli F, Proserpio P, Morrone E, Sartori I, Ferrara M, Gibbs SA, De Gennaro L, Lo Russo G, Nobili L (2016) Activation of the motor cortex during phasic rapid eye movement sleep. Ann Neurol 79:326–330.

De Gennaro L, Ferrara M, Ferlazzo F, Bertini M (2000) Slow eye movements and EEG power spectra during wake-sleep transition. Clin Neurophysiol 111:2107–2115.

Dockree PM, Kelly SP, Foxe JJ, Reilly RB, Robertson IH (2007) Optimal sustained attention is linked to the spectral content of background EEG activity: greater ongoing tonic alpha (approximately 10 Hz) power supports successful phasic goal activation. Eur J Neurosci 25:900–907.

Ermis U, Krakow K, Voss U (2010) Arousal thresholds during human tonic and phasic REM sleep. J Sleep Res 19:400–406.

Frauscher B, Joshi S, von Ellenrieder N, Nguyen DK, Dubeau F, Gotman J (2018) Sharply contoured theta waves are the human correlate of pontogeniculo-occipital waves in the primary visual cortex. Clin Neurophysiol 129:1526–1533.

Gonzalo-Ruiz A, Sanz-Anquela MJ, Lieberman AR (1995) Cholinergic projections to the anterior thalamic nuclei in the rat: a combined retrograde tracing and choline acetyl transferase immunohistochemical study. Anat Embryol (Berl) 192:335–349.

Gross DW, Gotman J (1999) Correlation of high-frequency oscillations with the sleep-wake cycle and cognitive activity in humans. Neuroscience 94:1005–1018.

Hartikainen KM, Sun L, Polvivaara M, Brause M, Lehtimäki K, Haapasalo J, Möttönen T, Väyrynen K, Ogawa KH, Öhman J, Peltola J (2014) Immediate effects of deep brain stimulation of anterior thalamic nuclei on executive functions and emotion–attention interaction in humans. J Clin Exp Neuropsychol 36:540–550.

Headley DB, Pare D (2013) In sync: gamma oscillations and emotional memory. Front Behav Neurosci 7:170.

Hutchison IC, Rathore S (2015) The role of REM sleep theta activity in emotional memory. Front Psychol 6:1439.

Jabbi M, Kohn PD, Nash T, Ianni A, Coutlee C, Holroyd T, Carver FW, Chen Q, Cropp B, Kippenhan JS, Robinson SE, Coppola R, Berman KF

(2015) Convergent BOLD and beta-band activity in superior temporal sulcus and frontolimbic circuitry underpins human emotion cognition. Cereb Cortex 25:1878–1888.
Jasper H (1958) Report of the committee on methods of clinical examination in electroencephalography. Electroencephalogr Clin Neurophysiol 10:370–375.
Jouny C, Chapotot F, Merica H (2000) EEG spectral activity during paradoxical sleep: further evidence for cognitive processing. Neuroreport 11:3667–3671.
Ketz NA, Jensen O, O'Reilly RC (2015) Thalamic pathways underlying prefrontal cortex–medial temporal lobe oscillatory interactions. Trends Neurosci 38:3–12.
Lachaux J-P, Rodriguez E, Martinerie J, Varela FJ (1999) Measuring phase synchrony in brain signals. Hum Brain Mapp 8:194–208.
Liu Z, de Zwart JA, Yao B, van Gelderen P, Kuo L-W, Duyn JH (2012) Finding thalamic BOLD correlates to posterior alpha EEG. Neuroimage 63:1060–1069.
Luppi PH, Clément O, Sapin E, Gervasoni D, Peyron C, Léger L, Salvert D, Fort P (2011) The neuronal network responsible for paradoxical sleep and its dysfunctions causing narcolepsy and rapid eye movement (REM) behavior disorder. Sleep Med Rev 15:153–163.
Lyamin OI, Kosenko PO, Korneva SM, Vyssotski AL, Mukhametov LM, Siegel JM (2018) Fur seals suppress REM sleep for very long periods without subsequent rebound. Curr Biol 28:2000–2005.e2.
Makeig S, Inlow M (1993) Lapses in alertness: coherence of fluctuations in performance and EEG spectrum. Electroencephalogr Clin Neurophysiol 86:23–35.
Manzano GM, Ragazzo PC, Tavares SM, Marino R Jr (1986) Anterior zygomatic electrodes: a special electrode for the study of temporal lobe epilepsy. Stereotact Funct Neurosurg 49:213–217.
Maris E, Oostenveld R (2007) Nonparametric statistical testing of EEG-and MEG-data. J Neurosci Methods 164:177–190.
Miyauchi S, Misaki M, Kan S, Fukunaga T, Koike T (2009) Human brain activity time-locked to rapid eye movements during REM sleep. Exp Brain Res 192:657–667.
Moroni F, Nobili L, Curcio G, Carli FD, Fratello F, Marzano C, Gennaro LD, Ferrillo F, Cossu M, Francione S, Russo GL, Bertini M, Ferrara M (2007) Sleep in the human hippocampus: a stereo-EEG study. PLoS One 2:e867.
Moroni F, Nobili L, De Carli F, Massimini M, Francione S, Marzano C, Proserpio P, Cipolli C, De Gennaro L, Ferrara M (2012) Slow EEG rhythms and inter-hemispheric synchronization across sleep and wakefulness in the human hippocampus. Neuroimage 60:497–504.
Muzur A, Pace-Schott EF, Hobson JA (2002) The prefrontal cortex in sleep. Trends Cogn Sci 6:475–481.
Nishida M, Uchida S, Hirai N, Miwakeichi F, Maehara T, Kawai K, Shimizu H, Kato S (2005) High frequency activities in the human orbitofrontal cortex in sleep-wake cycle. Neurosci Lett 379:110–115.
Oostenveld R, Fries P, Maris E, Schoffelen JM (2011) FieldTrip: open source software for advanced analysis of MEG, EEG, and invasive electrophysiological data. Comput Intell Neurosci 2011:1–9.
Paré D, Collins DR, Pelletier JG (2002) Amygdala oscillations and the consolidation of emotional memories. Trends Cogn Sci 6:306–314.
Price LJ, Kremen I (1980) Variations in behavioral response threshold within the REM period of human sleep. Psychophysiology 17:133–140.
Renouard L, Billwiller F, Ogawa K, Clément O, Camargo N, Abdelkarim M, Gay N, Scoté-Blachon C, Touré R, Libourel PA, Ravassard P, Salvert D, Peyron C, Claustrat B, Léger L, Salin P, Malleret G, Fort P, Luppi PH (2015) The supramammillary nucleus and the claustrum activate the cortex during REM sleep. Sci Adv 1:e1400177.
Rosenzweig I, Fogarasi A, Johnsen B, Alving J, Fabricius M, Scherg M, Neufeld M, Pressler R, Kjaer T, W van E B, Beniczky S (2014) Beyond the double banana: improved recognition of temporal lobe seizures in long-term EEG. J Clin Neurophysiol 31:1–9.
Sadaghiani S, Scheeringa R, Lehongre K, Morillon B, Giraud AL, Kleinschmidt A (2010) Intrinsic connectivity networks, alpha oscillations, and tonic alertness: a simultaneous electroencephalography/functional magnetic resonance imaging study. J Neurosci 30:10243–10250.
Sallinen M, Kaartinen J, Lyytinen H (1996) Processing of auditory stimuli during tonic and phasic periods of REM sleep as revealed by event-related brain potentials. J Sleep Res 5:220–228.
Saper CB, Scammell TE, Lu J (2005) Hypothalamic regulation of sleep and circadian rhythms. Nature 437:1257–1263.
Simor P, Gombos F, Szakadát S, Sándor P, Bódizs R (2016) EEG spectral power in phasic and tonic REM sleep: different patterns in young adults and children. J Sleep Res 25:269–277.
Simor P, Gombos F, Blaskovich B, Bódizs R (2018) Long-range alpha and beta and short-range gamma EEG synchronization distinguishes phasic and tonic REM periods. Sleep 41.
Simor P, van Der Wijk G, Gombos F, Kovács I (2019) The paradox of rapid eye movement sleep in the light of oscillatory activity and cortical synchronization during phasic and tonic microstates. Neuroimage 202:116066.
Simor P, van der Wijk G, Nobili L, Peigneux P (2020) The microstructure of REM sleep: why phasic and tonic? Sleep Med Rev 52:101305.
Sweeney-Reed CM, Zaehle T, Voges J, Schmitt FC, Buentjen L, Kopitzki K, Esslinger C, Hinrichs H, Heinze HJ, Knight RT, Richardson-Klavehn A (2014) Corticothalamic phase synchrony and cross-frequency coupling predict human memory formation. Elife 3:e05352.
Takahara M, Nittono H, Hori T (2002) Comparison of the event-related potentials between tonic and phasic periods of rapid eye movement sleep. Psychiatry Clin Neurosci 56:257–258.
Takahara M, Nittono H, Hori T (2006) Effect of voluntary attention on auditory processing during REM sleep. Sleep 29:975–982.
Tan X, Campbell IG, Feinberg I (2001) A simple method for computer quantification of stage REM eye movement potentials. Psychophysiology 38:512–516.
Tarokh L, Carskadon MA, Achermann P (2010) Developmental changes in brain connectivity assessed using the sleep EEG. Neuroscience 171:622–634.
van der Helm E, Yao J, Dutt S, Rao V, Saletin JM, Walker MP (2011) REM sleep de-potentiates amygdala activity to previous emotional experiences. Curr Biol 21:2029–2032.
Vertes RP, Albo Z, Viana Di Prisco G (2001) Theta-rhythmically firing neurons in the anterior thalamus: implications for mnemonic functions of Papez's circuit. Neuroscience 104:619–625.
Vinck M, Oostenveld R, Van Wingerden M, Battaglia F, Pennartz CM (2011) An improved index of phase-synchronization for electrophysiological data in the presence of volume-conduction, noise and sample-size bias. Neuroimage 55:1548–1565.
Voges BR, Schmitt FC, Hamel W, House PM, Kluge C, Moll CKE, Stodieck SR (2015) Deep brain stimulation of anterior nucleus thalami disrupts sleep in epilepsy patients. Epilepsia 56:e99–e103.
Walker MP (2009) The role of sleep in cognition and fmotion. Ann NY Acad Sci 1156:168–197.
Waterman D, Elton M, Hofman W, Woestenburg JC, Kok A (1993) EEG spectral power analysis of phasic and tonic REM sleep in young and older male subjects. J Sleep Res 2:21–27.
Wehrle R, Kaufmann C, Wetter TC, Holsboer F, Auer DP, Pollmächer T, Czisch M (2007) Functional microstates within human REM sleep: first evidence from fMRI of a thalamocortical network specific for phasic REM periods. Eur J Neurosci 25:863–871.
Xiao D, Barbas H (2002) Pathways for emotions and memory II. Afferent input to the anterior thalamic nuclei from prefrontal, temporal, hypothalamic areas and the basal ganglia in the rhesus monkey. THL 2:33–48.
Zotev V, Misaki M, Phillips R, Wong CK, Bodurka J (2018) Real-time fMRI neurofeedback of the mediodorsal and anterior thalamus enhances correlation between thalamic BOLD activity and alpha EEG rhythm. Hum Brain Mapp 39:1024–1042.